Mineral. Soc. Amer. Spec. Pap. **3**, 33–49 (1970).

PARTIAL FUSION PRODUCTS IN ALPINE-TYPE PERIDOTITES: SERRANIA DE LA RONDA AND OTHER EXAMPLES

John S. Dickey, Jr.
Smithsonian Astrophysical Observatory, Cambridge, Massachusetts 02138

Abstract

Mafic layers (1 cm to 2 m thick) in alpine-type peridotites of the Serrania de la Ronda (Betic Cordillera, Spain), Etang de Lers (Pyrenees, France), and Beni Bouchera (Er Rif, Morocco) are of two types, called here magmatic and tectonic.

Tectonic-type mafic layers, typically pyroxenites composed of minerals which are indigenous to the peridotite, may form several cross-cutting generations of layers and are believed to form by solid differentiation of deforming peridotite.

Magmatic-type mafic layers, composed of minerals which are often not stable constituents of the peridotite, vary from garnet pyroxenites to olivine gabbros. Chemically they are between basaltic and ultrabasic, typically with normative hypersthene (rarely nepheline). Physically they resemble tectonic-type layers; however, they have sharper contacts and form only one generation of layers.

A sequence of five mineral assemblages, compatible with crystallization (or recrystallization) along a decreasing $P-T$ gradient, has been found in magmatic-type layers of the Ronda massif:

I. gn+cpx±green sp (ceylonite)
II. gn+cpx+plag±green sp
III. cpx+green sp+plag±opx
IV. cpx+plag+ol+opx+brown sp (picotite)
V. cpx+plag+ol+opx+chr.

Peridotite amongst magmatic-type mafic layers in the Ronda massif is relatively depleted in Si, Al, Ca, and alkalies and relatively enriched in Mg, Ni, and Fe. The Fe enrichment, noticeable in olivine, orthopyroxene and bulk compositions, is attributed to equilibration between cooling magmatic-type mafic layers and adjacent peridotite.

Field relationships, petrographic textures, and chemical data suggest that magmatic-type layers formed from basic magmas produced by partial fusion of rising masses of peridotite.

Introduction

Statement of problem. The peridotite bodies which we now call the alpine type (Benson, 1926; Hess, 1955; Thayer, 1960) have been studied by petrologists for nearly two centuries. Today they are generally regarded as solid, or nearly solid, tectonic inclusions of mantle material. There are, however, conflicting views of their actual formation. Two prominent hypotheses invoke fundamentally different phenomena: fractional crystallization and partial fusion. The first hypothesis, proposed by Bowen (1928) and extended recently by Thayer, involves "gravity stratification of peridotite and gabbro in the upper part of the mantle and their later reemplacement together as crystal mushes" (Thayer, 1967, p. 238). The second hypothesis, advocated by Green and Ringwood (1967a) and others, suggests that these peridotites are the solid residue left after incomplete melting of upper mantle rock. This paper presents evidence that the formation of alpine-type peridotites is dominated by partial fusion.

Many alpine-type peridotite bodies contain mafic[1] layers, not, I believe, as a consequence of crystal sedimentation, but as the result of two different processes: segregation of minerals during deformation of solid peridotite and coalescence, also during deformation, of droplets formed by partial fusion. In accordance with this *interpretation* the two varieties will be referred to as tectonic- and magmatic-type mafic layers. In this paper, field, petrographic and chemical data from a study of mafic layers in peridotite bodies of the Serrania de la Ronda (Betic Cordillera, Spain), Beni Bouchera (Er Rif, Morocco), and Etang de Lers (central Pyrenees, France) will be presented with additional data and descriptions from the literature (Fig. 1).

Previous work. The basis for this study was laid by a multitude of scientists, many of whom are cited below. Work by the following geologists was especially important to the field study: A. Lacroix (1894, 1900) and H. G. Avé Lallemant (1967) at Etang de Lers, D. Orueta (1917) in the Serrania de la Ronda, and Y. Milliard (1959) and J. Kornprobst (1966) at Beni Bouchera.

General Characteristics of Mafic Layering

Tectonic-type mafic layers. Tectonic layering is a foliation, manifested by layers, boudins, and schlieren of spinel, pyroxenite[2]. These layers are common in alpine-type peridotites; they resist weathering and highlight the structure of the peridotite. There may be several, cross-cutting generations of tectonic-type layers in a peridotite body. They may be formed during deformation of the peridotite as the more easily deformed olivine is segregated from the pyroxenes and spinel. The most characteristic feature of these tectonic-type mafic layers is that their constituent minerals

---

[1] In this paper the term mafic does not include ultramafic rocks.

[2] Garnet peridotite would contain garnet rather than spinel in its tectonic-type mafic layers. Some garnet pyroxenite xenoliths in kimberlites may be of this type. Alpine-type peridotites, however, are typically spinel peridotites; garnets in them are usually derived from magmatic-type mafic layers.

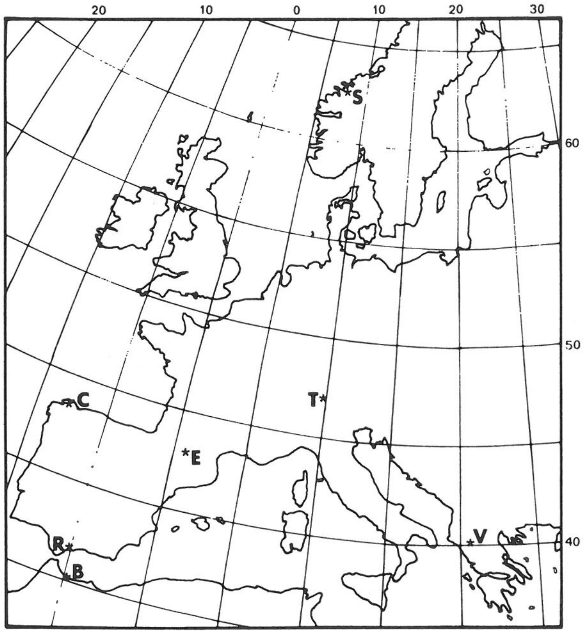

FIG. 1. Index map of localities mentioned in the text. Key: B = Beni Bouchera, Morocco; C = Cabo Ortegal, Spain; E = Etang de Lers, France; R = Serrania de la Ronda, Spain; S = Sondmör, Norway; T = Totalp, Switzerland; V = Vourinos, Greece.

are chemically similar to pyroxenes and spinels in the peridotite.

Magmatic-type mafic layers. Magmatic-type mafic layers form parallel sheets (1 cm to 2 m thick) which may extend for several hundred meters before pinching out. Like tectonic layers, the magmatic layers are confined and, therefore, indigenous to the peridotites. In the field layers of similar thickness usually occur together: one seldom finds a random mixture of thick and thin layers.

Between magmatic-type layers the peridotite is, typically, homogeneous dunite (ol+sp) or harzburgite (ol+opx+sp) with or without tectonic-type layers. Rarely, compositional banding is apparent: the peridotite changes from dunite or harzburgite to lherzolite (ol+opx+cpx+sp) with increasing distance from the nearest magmatic-type layer.

Compositions of magmatic-type mafic layers are between ultrabasic and basaltic. An average analysis contains 47 percent SiO_2, 14 percent Al_2O_3, 7 percent total iron as FeO, 17 percent MgO, 12 percent CaO and 1 percent Na_2O.

Mineralogically, magmatic-type layers range from garnet pyroxenites to olivine gabbros. There are five common mineral assemblages:

I. gn+cpx±green sp (ceylonite)
II. gn+cpx+plag±green sp
III. cpx+plag+green sp±opx
IV. cpx+plag+ol+opx+brown sp (picotite)
V. cpx+plag+ol+opx+chr.

In the Serraina de la Ronda peridotite massif all five assemblages are found. The other peridotite bodies which were studied contain three assemblages or less.

Magmatic layers often display a gneissic texture with compositional banding, preferred orientation and deformation of crystals. Where there has been little or no late deformation of the peridotite this gneissic foliation parallels the layering, and a conformable foliation can usually be found in the peridotite. Later deformations may create a foliation in the magmatic layer which is not parallel to the layering. In such cases the layer contacts have a saw-toothed appearance due to the intersection of the young foliation and the layer. Gneissic textures are not ubiquitous, however; some specimens, especially those from the interiors of thick layers, have undeformed, subhedral-granular textures.

Magmatic layers are less common than tectonic layers in alpine-type peridotites. They are often rare or absent. The peridotite bodies described below are remarkable for the abundance of magmatic-type mafic layers.

FIELD AND PETROGRAPHIC RELATIONSHIPS

Serrania de la Ronda

1. *Regional setting.* The Betic Cordillera (Fig. 2) contains three zones (Fontboté, 1966): the pre-Betic zone, a mildly deformed terrane of Mesozoic and younger, continental and shallow marine sediments; the sub-Betic zone, a region of northward thrust and folded, Mesozoic, pelagic sediments and lavas; and the Betic zone, a structurally complex association of igneous, metamorphic and sedimentary rocks of Paleozoic and younger age. Within the Betic zone the peridotite massif of the Serrania de la Ronda covers 300 km^2 near the Mediterranean coast between Estepona and Marbella (36° 40″ N. Lat., 5° W. Long.).

2. *Local environment.* The Ronda massif (Fig. 3) is surrounded by marbles, gneisses and hornfelses which increase in metamorphic grade toward the peridotite.[1]

Metamorphosed sediments are exposed in valleys within the massif and form isolated masses lying on the peridotite. In some respects, therefore, the massif resembles an elliptical (38×12 km) sheet with metasediments above and below and a maximum exposed thickness of 1.2 km. The contact around the peridotite massif is consistently steep, however, suggesting that peridotite extends below the surface. Preliminary gravity measurements (T. Loomis, pers. commun.) suggest that the peridotite extends southward beneath the coastal plain.

The peridotite contact is typically a sheared surface between country rock and serpentinite. The serpentinite varies in thickness from a few meters to several hundred meters. Breccia of rounded serpentinite blocks in a disrupted serpentinite matrix is common along the contact and occurs also in Miocene sediments near the coast. This

---

[1] T. Loomis of Princeton University is currently studying the metamorphic and structural environment of the Ronda massif.

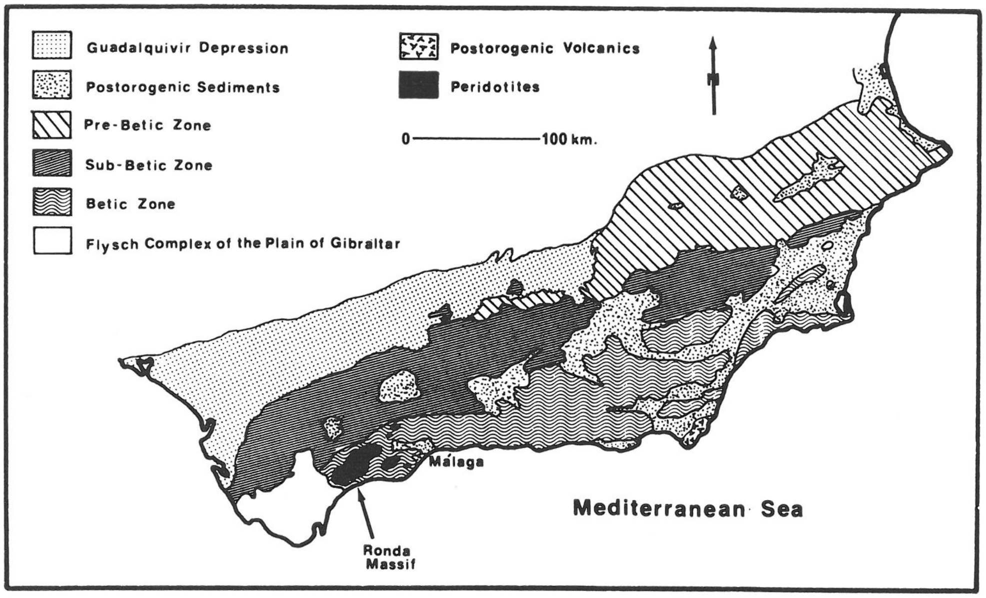

FIG. 2. Simplified geological map of the Betic Cordillera (modified after Fontobté, 1966).

brecciation may be due to slumping, crushing, or gas explosions.

Metamorphic and structural complications obscure the time of peridotite emplacement; however, Triassic sediments have been found along the northeast contact (Fallot, 1948), so a post-Triassic date is probable.

3. *Peridotite and mafic layers.* The massif is 85 to 90 percent peridotite; harzburgite is the most abundant variety, followed by dunite and lherzolite. These grade from one to another with no apparent regularity except that amongst magmatic-type mafic layers lherzolite is rare and dunite common. In general the peridotite contains xenomorphic orthopyroxene (En_{85-91}) and clinopyroxene grains (2 mm) in a ground-mass of polygonal olivine (Fo_{86-91}) grains (1 mm) with interstitial brown to opaque spinel. Calcic plagioclase commonly surrounds embayed spinel grains and, rarely, forms interstitial grains. The degree of cataclasis varies: some specimens are mylonites; others appear almost undeformed. Common secondary minerals in the peridotite are thomsonite, in veinlets, and serpentine (chrysotile). The degree of serpentinization is low. Massive serpentinite is found only near the margins of the massif and in restricted fracture zones. Compared to most alpine-type peridotites the Ronda massif is remarkably anhydrous besides the occurrences of massive serpentine, hydrous minerals are common only in felsic veins which intrude the massif.

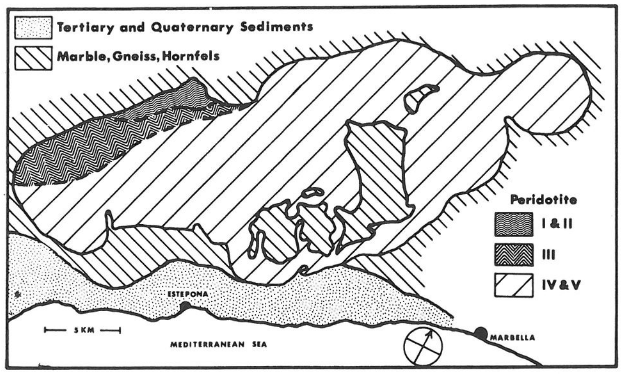

FIG. 3. Geological sketch map of the Serrania de la Ronda. The peridotite is subdivided according to the mineral assemblages found in magmatic-type mafic layers.

Tectonic and magmatic-type mafic layers are common in the Ronda massif. Often they are parallel, but there are foliations (tectonic layers) which crosscut the magmatic layers. The magmatic layers are unevenly distributed: some parts of the massif lack them altogether, elsewhere there are interlayered sections with as much as 37 percent mafic material. Typically, magmatic layers constitute 10 to 20 percent of the rock.

The magmatic layering defines simple structures in the peridotite. The layers change attitude gradually or so abruptly as to imply faulting. Abrupt changes are found across zones of intense serpentinization and fracturing. Tight folding of the magmatic layering has not been observed.

Compared to peridotite the mafic layers are, when completely crystallized, strong, hard and rigid; consequently, they deform by fracturing rather than by plastic flow or mylonitization. This difference in mechanical properties has apparently resulted in a rectangular joint pattern (Fig. 4) which is found in most magmatic layers and in some tectonic layers but dies out immediately in the adjacent peridotite. Although they are not polygonal, the joints are reminiscent of columnar joints in igneous rocks, and thermal contraction may, in fact, have widened them.

Initially, however, they were probably extension fractures.

4. *Mineral assemblages in the magmatic layers.* The complete sequence of five mineral assemblages, from garnet pyroxenite to olivine gabbro, is represented in the magmatic-type mafic layers of the Ronda massif. Their regional distribution (Fig. 3) is orderly. Proceeding, roughly, from west to east one encounters assemblages I through V. The changes from one assemblage to another are gradual; however, a regional pattern is evident: assemblages I and II have not been found with assemblages IV and V.

It is difficult to ascertain how much of the observed variation in mineralogy is primary and how much is due to subsolidus reactions. All of the magmatic layers studied have been changed by subsolidus reactions, and the direction of change has been from assemblage I (garnet pyroxenite) toward assemblage V (olivine gabbro). Looking beyond the overprint of subsolidus change, however, petrographic evidence suggests that assemblages I, III, and V crystallized directly from magmas.

Layers of assemblage I (gn+cpx+sp) have been found only near the northwest margin of the massif, in the vicinity of Jubrique. They are thin (<5 cm), sparse, and substantially altered to an assemblage of plagioclase, pyroxene, spinel and amphibole.

Layers of assemblage II (gn+cpx+plag±sp) are thicker (up to 80 cm) and more abundant than those of assemblage I. Assemblage II may also be a primary assemblage in the Ronda massif, but the uneven texture, created by large, embayed garnets lying in a finer-grained matrix of clinopyroxene and plagioclase (Fig. 5), suggests that it formed by recrystallization of assemblage I. If so, the following reactions may be pertinent:[1]

FIG. 4. Magmatic-type mafic layer in the Serrania de la Ronda peridotite massif. Note the rectangular joint pattern in the mafic layer and the foliation in the overlying peridotite.

1. $\underset{\text{gn}_{\text{I}}}{(\text{Mg, Fe})_3\text{Al}_2\text{Si}_3\text{O}_{12}} + \underset{\text{cpx}_{\text{I}}}{\text{NaAlSi}_2\text{O}_6}$

$$\rightarrow \underset{\text{plag}_{\text{II}}}{\text{NaAlSi}_3\text{O}_8} + \underset{\text{sp}_{\text{II}}}{(\text{Mg, Fe})\text{Al}_2\text{O}_4} + \underset{\text{cpx}_{\text{II}}}{(\text{Mg, Fe})_2\text{Si}_2\text{O}_6}$$

2. $\underset{\text{gn}_{\text{I}}}{(\text{Mg, Fe})_3\text{Al}_2\text{Si}_3\text{O}_{12}} + \underset{\text{cpx}_{\text{II}}}{\text{CaAl}_2\text{SiO}_6}$

$$\rightarrow \underset{\text{plag}_{\text{II}}}{\text{CaAl}_2\text{Si}_2\text{O}_8} + \underset{\text{sp}_{\text{II}}}{(\text{Mg, Fe})\text{Al}_2\text{O}_4} + \underset{\text{cpx}_{\text{II}}}{(\text{Mg, Fe})_2\text{Si}_2\text{O}_6}$$

3. $\underset{\text{gn}_{\text{II}}}{2\text{Ca}_{0.5}(\text{Fe, Mg})_{2.5}\text{Al}_2\text{Si}_3\text{O}_{12}}$

$$\rightarrow \underset{\text{plag}_{\text{II}}}{\text{CaAl}_2\text{Si}_2\text{O}_8} + \underset{\text{sp}_{\text{II}}}{(\text{Fe, Mg})\text{Al}_2\text{O}_4} + \underset{\text{cpx}_{\text{II}}}{2(\text{Fe, Mg})_2\text{Si}_2\text{O}_6}$$

Each of the above reactions produces spinel, yet spinel is rare or absent in the assemblage II layers. A chemical analysis (Table 4, analysis b) suggests that the spinel may be dissolved in the clinopyroxene.

Magmatic layers in 80 percent of the Ronda massif are of assemblages III, IV and V. Layers of assemblage III (cpx+sp+plag±opx) may be primary. They are composed (Fig. 6) of tightly interlocking pyroxenes with interstitial spinel and plagioclase much of which may have exsolved from pyroxene. There is no evidence of a preceding garnetiferous assemblage.

The clinopyroxenes of assemblage III crystallized with excess Mg, Fe, Al, and Cr which exsolved as spinel, forming rods parallel to the *c* axis of the host and sheets parallel to (010) and (100). Orthopyroxene lamellae also exsolved parallel to (100) of the clinopyroxene. After exsolving the spinel and orthopyroxene reacted with the host:

4. $\underset{\text{cpx host}}{[x\text{CaAl}_2\text{SiO}_6 \cdot y\text{NaAlSi}_2\text{O}_6]} + \underset{\text{opx lamellae}}{2(x+y)\text{MgSiO}_3}$

$$\rightarrow \underset{\text{plag}}{[x\text{CaAl}_2\text{Si}_2\text{O}_8 \cdot y\text{NaAlSi}_3\text{O}_8]} + \underset{\text{ol}}{(x+y)\text{Mg}_2\text{SiO}_4}$$

5. $\underset{\text{cpx host}}{[\text{CaMgSi}_2\text{O}_6 \cdot \text{Mg}_2\text{Si}_2\text{O}_6]} + \underset{\text{exsolved sp}}{\text{MgAl}_2\text{O}_4}$

$$\rightarrow \underset{\text{plag}}{\text{CaAl}_2\text{Si}_2\text{O}_8} + \underset{\text{ol}}{2\text{Mg}_2\text{SiO}_4}$$

As a result of these reactions many clinopyroxene crystals now contain lamellae of plagioclase plus olivine (Fig. 7). An opaque oxide, magnetite or ilmenite, is also present in some of these lamellae. Since reactions 4 and 5 involve expansions of about 10 percent the host clinopyroxenes are now disrupted.

Assemblage IV is the most common assemblage in the magmatic-type mafic layers of the Ronda massif. It is a transitional assemblage, created by subsolidus reactions

---

[1] For simplicity complete mineral formulae are not used in these equations.

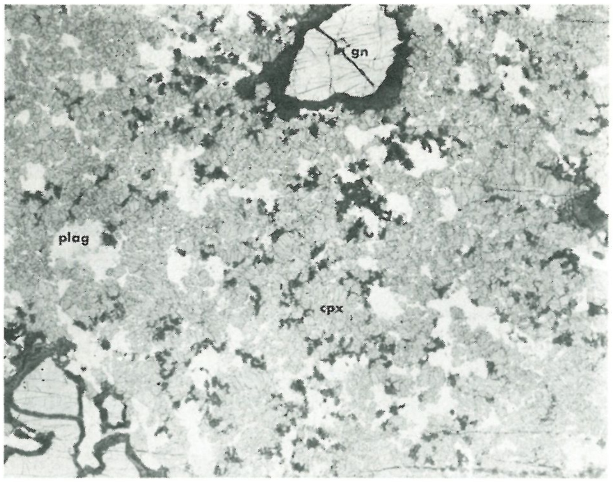

Fig. 5. Garnet plagioclase pyroxenite, R127, (Table 1, analysis b). Nonpolarized light. Field width: 22 mm.

Fig. 7. Lamellae of olivine+plagioclase parallel to (100) and spinel parallel to (010) in a clinopyroxene crystal of spinel pryoxenite, R251. Crossed polarized light. Field width: 1 mm.

changing spinel pyroxenite (assemblage III) into olivine gabbro (assemblage V). Assemblage IV is characterized by large, ragged pyroxenes surrounded by a medium-grained assemblage of olivine, plagioclase and pyroxene. This medium-grained assemblage formed from pre-existing pyroxene and spinel by reactions similar to 4 and 5.

In some assemblage IV rocks there are large orthopyroxenes containing plagioclase lamellae, exsolved parallel to (100) of the host. The absence of a mafic phase in these lamellae suggests that Al was originally incorporated into the orthopyroxene as Al_2SiO_5 (*cf.* O'Hara and Yoder, 1967) and exsolved with Ca by reaction 6:

6. $CaMgSi_2O_6 + Al_2SiO_5 \rightarrow CaAl_2Si_2O_8 + MgSiO_3$

Between assemblage III and V the spinel changes from ceylonite to chromite. This change is accomplished through the formation of new plagioclase and olivine by reactions in which the spinel participates. As these reactions proceed the spinel becomes enriched in Cr and Fe^{3+}. The typical spinel of assemblage IV is brown picotite, surrounded by a rim of plagioclase (Fig. 8). As the rims grow, the spinels become smaller amd more opaque.

Layers of assemblage V (cpx+plag+opx+ol+chr) probably crystallized as subhedral-granular gabbros and remained essentially unchanged by subsequent subsolidus reactions. There has been some exsolution in pyroxenes (op*x* exsolving from cp*x* and vice versa), but most crystals are homogeneous. Primary orthopyroxene, which is rare in assemblage III, is an abundant, essential phase of assemblage V, probably reflecting a lower temperature of crystallization.

This sequence of mineral assemblages encompasses all magmatic-type mafic layers encountered in the Ronda massif. Considerable variation exists, however, in modal

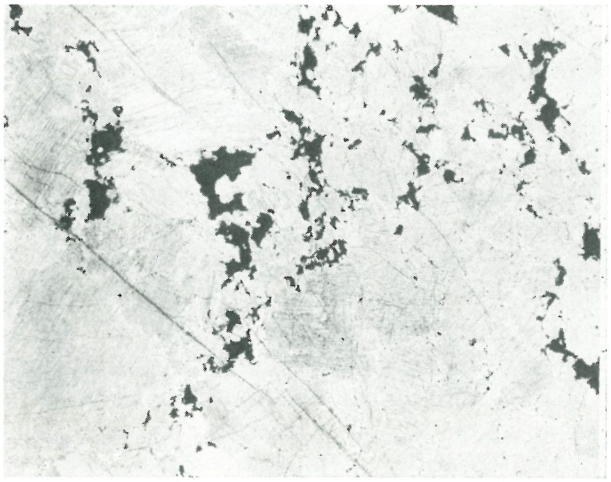

Fig. 6. Spinel pyroxenite, R251, (Table 1, analysis c) Nonpolarized light. Field width: 23 mm.

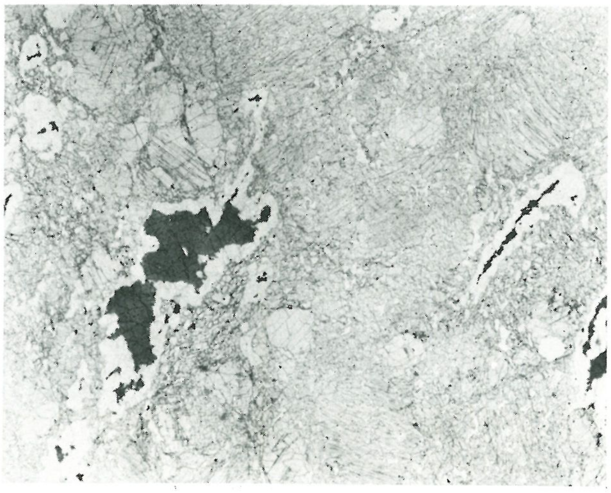

Fig. 8. Gabbro, R322, (Table 1, analysis f). Nonpolarized light. Field width: 21 mm.

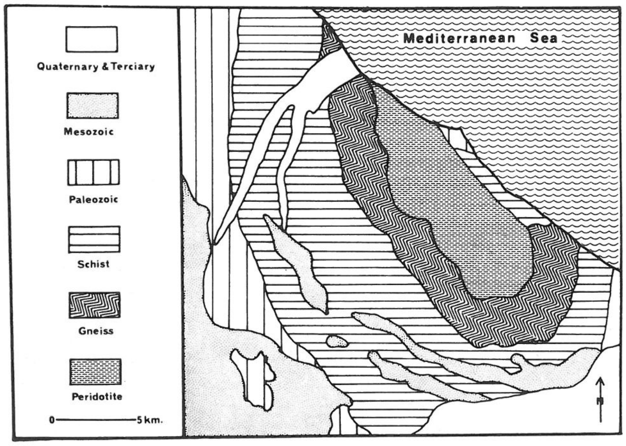

FIG. 9. Geological sketch map of the Beni Bouchera peridotite massif, Morocco (after Milliard, 1959).

and bulk chemical composition. These variations are discussed below.

The tectonic-type mafic layers (up to 1 m thick) are spinel pyroxenites, usually websterites rich in chrome diopside. They occur throughout the massif, associated with magmatic-type layers of all five mineral assemblages.

Beni Bouchera Massif

1. *Regional setting.* Geologically, as well as topographically, Er Rif of Morocco is nearly a mirror image of the Betic Cordillera. Southwestbound nappes and thrust sheets dominate the regional structure, which increases in complexity from southwest to northeast. The Beni Bouchera peridotite massif occupies 53 km² within a complex zone of Paleozoic and Triassic rocks along the coast between Bou Hamed and El Jebah (35° 22″ N. Lat., 4° 50″ W. Long.).

2. *Local environment.* The Beni Bouchera massif is surrounded (Fig. 9) by metamorphic rocks resembling the schist-gneiss terrane of the Ronda massif. The metamorphic grade increases toward the massif and may be related to the emplacement of the peridotite. Foliations in the country rocks (Milliard, 1959) and in the peridotite (Kornprobst, 1966) define a simple, domical structure, The gneiss-peridotite contact is a steep shear zone along which the peridotite is thoroughly serpentinized and commonly brecciated.

3. *Peridotite and mafic layers.* The peridotite is dominantly serpentinized harzburgite. It is distinctly banded due to magmatic amd tectonic-type mafic layers and rare bands (7 cm) of lherzolite. Occasionally two magmatic-type layers are separated by peridotite which changes from harzburgite near the mafic layers to lherzolite in the center.

The tectonic-type mafic layers are typically orthopyroxenites (*cf.* websterite in the Ronda massif).

The magmatic-type mafic layers (1 cm to 2 m thick) are garnet pyroxenites (assemblage I). Some magmatic layers are homogeneous, but others are zoned (Fig. 10). Typically, the garnet pyroxenite layers contain (Kornprobst, 1966) 60-65 percent clinopyroxene, 35-40 percent garnet, and minor amphibole and opaques. There has been substantial recrystallization of the garnet pyroxenite assemblage to clinopyroxene, green spinel, plagioclase and olivine.

In addition to clearly defined mafic layers, there are in the peridotite thin layers and fragments or isolated minerals of the garnet pyroxenite. The presence of garnet crystals in the peridotite led Milliard (1959) to describe it as garnetiferous saxonite (harzburgite). Actually the peridotite is a spinel-bearing harzburgite, and, as Kornprobst suggests (1966) the garnets were mechanically derived by deformation and fragmentation of garnet pyroxenite layers. There is a continuous gradation from thin layers through small lenses (boudins) to isolated crystals in the peridotite.

Etang de Lers

1. *Regional setting.* In the Pyrenees, a crystalline core of Paleozoic rocks is mantled to the north and south by Mesozoic and, further outwards, Cenozoic sediments. Peridotite appears only in a narrow, 200 km long zone of tightly folded Mesozoic sediments, bounded to the south by the north Pyrenean fault and to the north by satellite massifs (De Sitter, 1956) of Paleozoic granite and gneiss in the northern Mesozoic zone. The peridotite forms isolated, randomly oriented blocks (Avé Lallemant, 1967) concentrated on the northern side of the narrow zone and accompanied by increasingly intense metamorphism and brecciation. One such block is the type locality of lherzolite

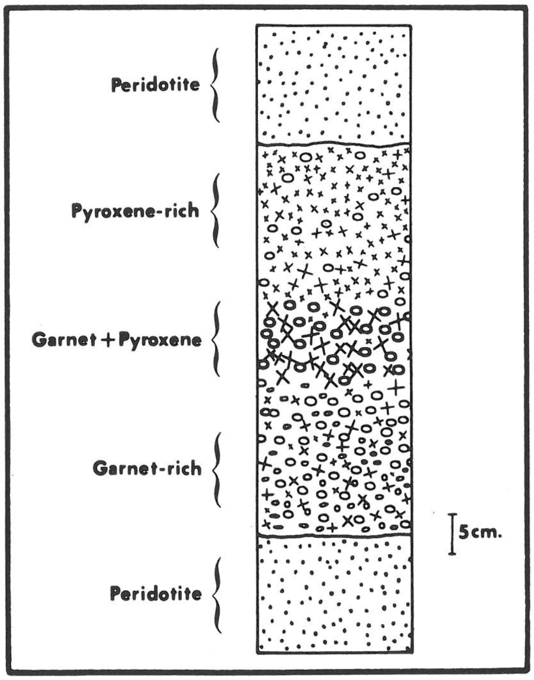

FIG. 10. Zoned garnet pyroxenite layer in serpentinized peridotite of the Beni Bouchera massif. Clinopyroxenes (x) and garnets (o) are concentrated in zones along the upper and lower contacts, respectively. Grainsize increases toward the center of the layer. (Drawn from field notes.)

(de Lâmetherie, 1795) at Etang de Lers (42° 45″ N. Lat., 1° 40″ E. Long.).

2. *Local environment.* The Etang de Lers peridotite body (1.6×0.7 km) lies in a pre-Cenomanian syncline of Aptian-Albian marble (Collée, 1963) (Fig. 11). Massive marble and peridotite are separated by breccia, created probably (Ravier, 1959) by gas explosions. During brecciation, fine-grained peridotitic material with few fragments of carbonate appears to have been in a fluidized condition, forming multiple-injection, microbreccia dikes and net veins in larger pieces of marble and peridotite. Breccia zones, containing little or no carbonate, are present within the peridotite body. The explosion breccia contains only peridotite and Aptian-Albian marble and must have formed during or after the emplacement of the peridotite in these carbonates. A regional association with basic igneous rocks of Cretaceous age (Zwart, 1953) and a K-Ar age of 116±5 m.y. for a hornblendite vein in the peridotite (Avé Lallemant, 1967) indicate that the emplacement occurred during the middle Cretaceous.

3. *Peridotite and mafic layers.* The Etang de Lers body is dominantly lherzolite with abundant tectonic-type spinel pyroxenite layers. Zones of harzburgite, up to 20 m thick, are found parallel to the tectonic type pyroxenite layers (Avé Lallemant, 1967). Some of these pyroxenite layers are zoned: an unusual variety has clinopyroxene concentrated along one or both margins; more common are layers with olivine-rich centers and pyroxene-rich margins. In places the tectonic layers are tightly folded; such folding is not shown by the magmatic layering.

The five magmatic-type mafic layers (30 to 40 cm thick) in the Etang de Lers peridotite body are garnet and spinel pyroxenites (assemblage I). They are compact, medium-grained (garnets to 4 mm, pyroxenes to 2 mm), anhedral-granular rocks with the following contact and internal features (*cf.* Avé Lallemant, 1967). Instead of lherzolite, the peridotite near (5 to 10 cm) the contact is dunite or harzburgite with brown spinel (picotite), little orthopyroxene, and little or no clinopyroxene. At the contact is a thin (2 mm) zone dominated by orthopyroxene with accessory brown spinel, clinopyroxene and secondary amphibole. Along the contact the mafic layer contains clinopyroxene with accessory orthopyroxene and brown spinel; within a few mm inwards the spinel changes to green (ceylonite). The clinopyroxene of the mafic layer is bright chromian green along the contact, but a few millimeters inwards it is a more subdued, grey green. Garnet is typically concentrated in the interiors of the layers. Many garnets are rimmed or replaced by a fine-grained assemblage of pyroxene, green spinel, plagioclase and amphibole. Green spinel occupies the interiors of some garnet crystals. This relationship may signify a change from a spinel-bearing to a garnet-bearing assemblage caused by cooling under pressure of 10 to 18 kbars (Fig. 15b). Orthopyroxene becomes less abundant and disappears completely in the interiors of some magmatic layers.

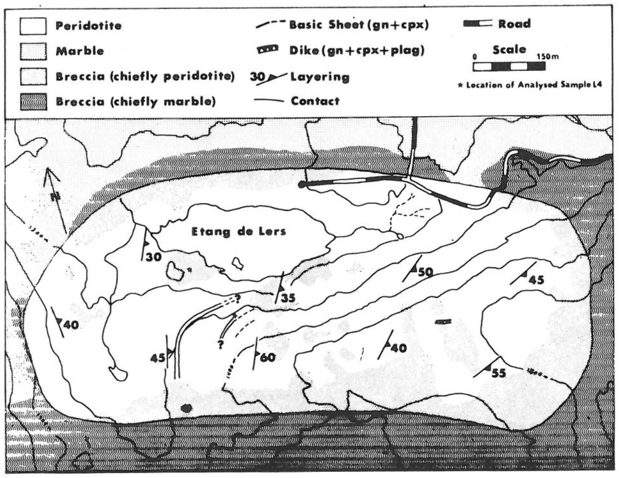

FIG. 11. Geological map of the peridotite body at Etang de Lers, French Pyrenees (after Avé Lallemant, 1967).

ANALYTICAL DATA

Methods of Analysis. Whole rock analyses were performed by E. Jarosewich of the U. S. National Museum, using a combination of gravimetric and instrumental methods.

Mineral analyses were performed on a MAC model 400 electron microprobe (15–20 kv, 0.01–0.025 μa) using a variety of natural and artificial mineral standards. The data were reduced by an iterative computer program (Probeg II) applying beam current drift, background, absorption, fluorescence, and dead time corrections. As a general rule, three significant figures are reported for amounts of 10 weight percent or more, two figures for amounts between 1 and 10 percent and one figure for amounts less than 1 percent.

Refractive indices were measured on a flat stage with Na light and simultaneous calibration by Abbé refractometer.

X-ray diffraction measurements were repeated several times on a Norelco x-ray diffractometer, using Cu Kα radiation, 1°–0.006″–1° collimating slits, and a scanning speed of 0.25° 2θ per minute.

Bulk compositions

1. *Mafic layers.* Bulk compositions of magmatic-type mafic layers (Table 1) are between basaltic and ultrabasic All are undersaturated, with normative olivine; most have normative hypersthene; but some are critically undersaturated, with nepheline in the norm. These compositions are characterized by high Ca, Al, and Mg (Figure 12) and low alkali contents. Similar compositions are characteristic of many basic xenoliths in the alkali olivine basalt suite and in kimberlites. Some cumulate hybrids (Wager and Brown, 1967) and parts of flow differentiated dikes (Gibb, 1968) are also similar.

If the magmatic-type mafic layers did originate by partial fusion of mantle rock, and if it were possible to analyze representative, unaltered products of the magmas, the bulk compositions would depend upon the composition of the starting material, the pressure during melting, and the amount of melting. Unfortunately, to this list of variables we must add the possibilities of partial loss of the original magma, post-crystallization alterations, and nonrepresentative sampling. Sampling bias may be a source of error: the

TABLE 1. CHEMICAL ANALYSES AND CIPW NORMS OF MAFIC LAYERS IN THE ETANG DE LERS AND SERRANIA DE LA RONDA PERIDOTITES

	a	b	c	d	e	f	g	h	i
Type	*M*(I)	*M*(II)	*M*(III)	*M*(III–IV)	*M*(III–IV)	*M*(IV)	*M*(V)	*M*(III–IV?)	*T?*
SiO_2	46.64	47.73	44.09	46.67	46.68	48.33	48.91	53.21	53.93
TiO_2	0.07	0.73	1.12	0.24	0.19	0.31	0.06	0.09	0.02
Al_2O_3	14.67	16.16	14.51	17.71	12.91	11.83	11.61	5.17	1.57
Cr_2O_3	0.23	0.00	0.06	0.09	0.25	0.47	0.35	0.82	1.83
Fe_2O_3	1.26	0.94	2.47	0.96	0.99	0.48	0.53	0.63	0.53
FeO	5.03	7.84	4.97	6.15	5.43	4.43	5.81	5.42	2.49
MnO	0.14	0.15	0.14	0.14	0.17	0.12	0.15	0.14	0.10
MgO	15.89	9.88	14.80	12.16	20.81	22.38	20.01	29.81	22.39
CaO	14.55	14.15	16.44	14.16	10.33	9.86	11.27	3.92	16.05
Na_2O	0.86	1.89	0.89	1.30	0.96	0.77	0.53	0.18	0.43
K_2O	<0.01	<0.01	0.01	<0.01	0.00	0.01	0.00	0.00	<0.01
H_2O^+	0.45	0.35	0.24	0.37	1.03	0.52	0.56	0.33	0.52
H_2O^-	0.15	0.06	0.09	0.06	0.10	0.11	0.09	0.11	0.10
P_2O_5	<0.01	0.00	0.00	0.00	0.00	0.00	0.00	0.00	0.00
NiO	0.05	<0.01	0.03	0.03	0.08	0.11	0.06	0.02	0.09
$SO_3^=$	<0.05	0.00	0.04	0.00	0.12	0.06	0.00	0.05	0.00
Total	99.99	99.88	99.90	100.04	100.05	99.79	99.94	99.90	100.05
Or	—	—	—	—	—	0.06	—	—	—
Ab	7.28	15.76	—	11.00	7.34	6.12	4.48	1.20	3.64
An	36.17	35.61	35.74	42.49	31.34	29.00	29.30	13.47	2.35
Ne	—	0.12	3.94	—	—	—	—	—	—
Di	28.59	28.02	35.69	22.25	15.76	15.70	21.12	4.71	60.48
Hy	2.20	—	—	1.23	14.13	23.30	25.47	69.96	27.20
Ol	22.85	17.19	18.13	20.66	27.98	22.90	17.51	7.74	2.26
Mt	1.83	1.36	3.58	1.39	1.44	0.70	0.77	0.91	0.77
Chr	0.34	—	0.09	0.13	0.37	0.69	0.52	1.21	2.70
Ilm	0.13	1.39	2.13	0.46	0.36	0.59	0.11	0.17	0.04
Rest	0.45	0.35	0.50	0.37	1.24	0.63	0.56	0.42	0.52
Total	99.84	99.82	99.80	99.98	99.95	99.68	99.85	99.79	99.95
$Na_2O + K_2O$	0.86	1.89	0.90	1.30	0.96	0.78	0.53	0.18	0.43
$\frac{FeO+Fe_2O_3}{MgO+FeO+Fe_2O_3}$	0.284	0.470	0.334	0.369	0.236	0.180	0.241	0.169	0.119

Key to Table 1

Type: *M* = magmatic, *T* = tectonic, Roman numerals stand for mineral assemblages (p. 34).

a. Garnet pyroxenite, L4, Etang de Lers, France. Mode: 72% cpx, 24% gn, <0.5% sp, 4% secondary.

b. Garnet-plagioclase pyroxenite, R127, Serrania de la Ronda, Spain. Mode: 61% cpx, 23% plag, 5% gn, 11% secondary.

c. Spinel pyroxenite, R251, Serrania de la Ronda. Mode: 81% cpx, 8% sp, 7% plag, 4% ol, <0.5% ilm.

d. Gabbro, R183, Serrania de la Ronda. Mode: 51% cpx, 30% plag, 15% ol, 3% sp, 0.6% chr, 0.4% opx.

e. Olivine gabbro, R120, Serrania de la Ronda. Mode: 23% cpx, 33% plag, 27% ol, 3% sp, 12% opx, 2% secondary.

f. Olivine gabbro, R322, Serrania de la Ronda. Mode: 35% cpx, 23% ol, 22% plag, 16% opx, 4% chr+sp, <0.5% secondary brown amphibole.

g. Olivine gabbro, R343, Serrania de la Ronda. Mode: 24% ol, 23% cpx, 15% opx, 36% plag, <1% chr.

h. Orthopyroxenite, R349, Serrania de la Ronda. Mode: 79% opx, 9% ol, 7% cpx, 4% plag, 1% sp.

i. Websterite, R301, Serrania de la Ronda. Mode: 64% cpx, 35% opx, 1% sp.

Analyst: E. Jarosewich, U. S. National Museum, Washington, D. C.

analyzed specimens were collected with emphasis on freshness; it is possible that pyroxene-rich portions of inhomogeneous layers were preferentially sampled. The effects of post-crystallization alteration have been slight, but the actual loss of volatile constituents from the crystallizing magmatic layers may have been significant. For example, K_2O in magmatic layers of the Ronda massif is typically less than 0.01 percent; if the magmatic layers truly represent protobasalts, K_2O would have to be enriched by two orders of magnitude in the formation of basalt. It is unlikely that any fractionation process which could accomplish this enrichment would produce basaltic abundances for the other elements. Given this many variables it may be foolish to look for regular variation patterns; yet, for mafic layers in the Ronda massif, a pattern does exist.

Magmatic-type mafic layers from the Ronda massif

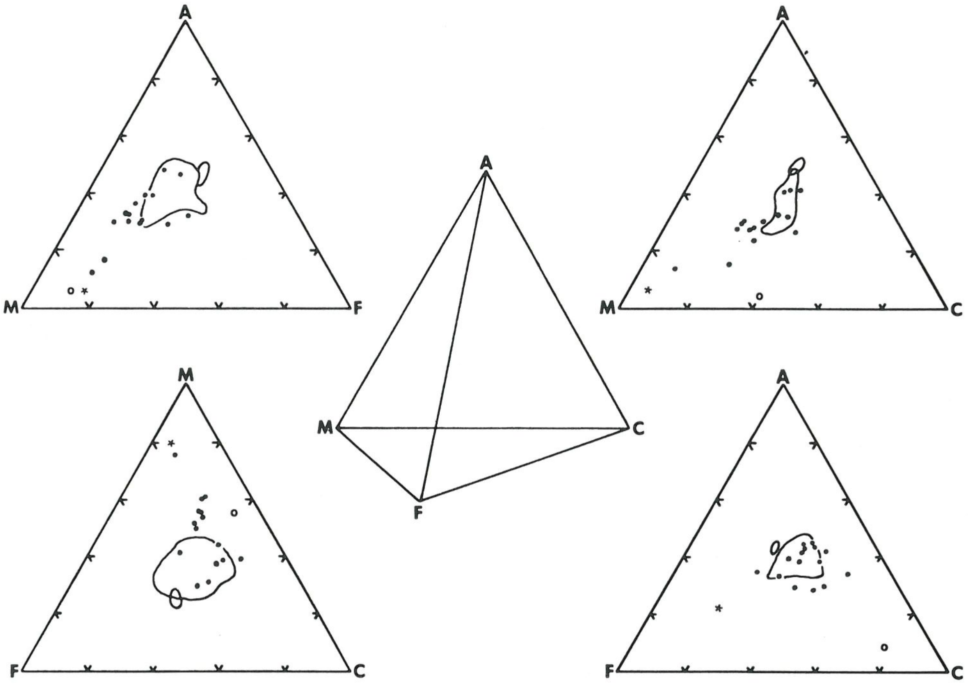

FIG. 12. Comparison in terms of weight percent A=Al_2O_3, C=CaO, M=MgO, and F=0.9 Fe_2O_3+FeO+MnO of magmatic-type mafic layers (•), a websterite layer R301, (○), an assortment of basic inclusions in volcanic rocks of the alkali olivine basalt suite (Lovering and White, 1968: Yoder and Tilley, 1962) shown as the larger outlined area, average basalts (Manson, 1967) shown as the smaller outlined area, and a peridotite (R224) (*).

(Fig. 13) follow a definite, though erratic, trend: as the Fe:Mg ratio increases Al, Ca, Na+K, Ti, Fe and Mn increase, Mg and Cr decrease.

The circled points in Figure 13 are for a 15-cm thick websterite layer (R301) in the peridotite (Table 1, analysis i). In the field this layer is part of a section of interlayered websterite and peridotite. The attitude of the layering conforms to that of magmatic-type mafic layers in the area. During field examination this layer was thought to be an unusually thick, tectonic-type mafic layer. The bulk and mineral compositions (discussed below), however, suggest that it may be an adcumulate (Wager and Wadsworth, 1960), formed by accumulation of pyroxenes in a magmatic layer and subsequent removal of the residual liquid.

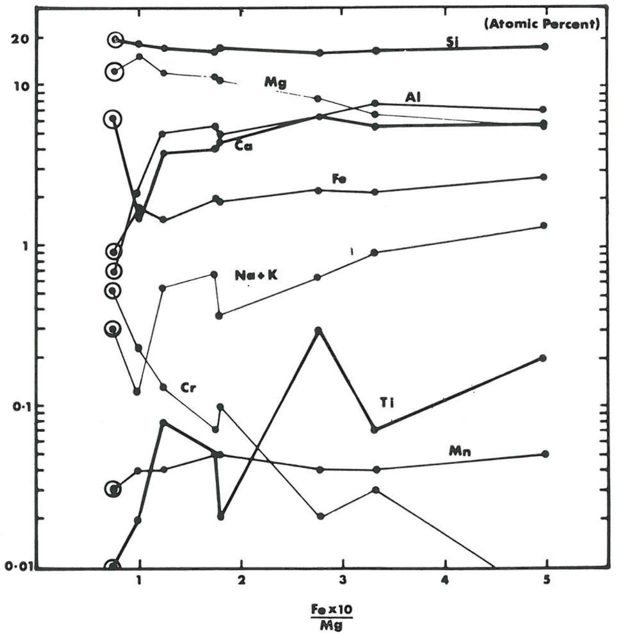

FIG. 13. Variation diagram, atomic percent of the element vs 10Fe/Mg, for magmatic-type mafic layers (•) and a websterite layer (⊙) of the Serrania de la Ronda peridotite massif.

The variation pattern in Figure 13 is not diagnostic of any single process. Such variation could be created by fractional crystallization, partial fusion, or varying amounts of leakage. The leakage possibility is difficult to assess; however, it seems unlikely because of the relatively constant Si concentration and the lack of any definite field evidence. There are in all of these peridotite massifs younger felsic intrusives, but these have not yet been related to the magmatic mafic layers. Fractional crystallization and partial fusion will be discussed below, following data on the peridotite compositions.

2. *Peridotites*. In the Ronda massif there is a range of peridotite compositions (Table 2) and a clear relationship between peridotite composition and the abundance of magmatic-type mafic layers. Figure 14 shows the major element variation in 3 peridotite samples from the Ronda massif. R131 was collected from a section which contains abundant magmatic-type mafic layers. R224 and R243 both came

TABLE 2. CHEMICAL ANALYSES OF PERIDOTITES FROM THE SERRANIA DE LA RONDA

	a	b	c
SiO_2	44.35	43.61	42.55
TiO_2	0.14	0.06	0.16
Al_2O_3	3.64	2.93	2.50
Cr_2O_3	0.33	0.39	0.36
Fe_2O_3	0.59	1.09	1.72
FeO	7.53	6.74	6.96
MnO	0.13	0.11	0.12
MgO	38.75	39.86	39.89
CaO	3.29	2.66	2.42
Na_2O	0.26	0.26	0.17
K_2O	0.00	0.01	0.00
H_2O^+	0.67	1.89	2.99
H_2O^-	0.06	0.15	0.16
P_2O_5	0.00	0.00	0.00
NiO	0.27	0.26	0.26
$SO_3^=$	0.12	0.03	0.00
Total	100.13	100.05	100.26
Na_2O+K_2O	0.26	0.27	0.17
$\frac{FeO+Fe_2O_3}{MgO+FeO+Fe_2O_3}$	0.173	0.164	0.179

Key to Table 2

a. Lherzolite, R243, from outcrop with no magmatic-type mafic layers.
b. Harzburgite, R224, from outcrop with no magmatic-type mafic layers.
c. Harzburgite, R131, from a section of interlayered peridotite and magmatic-type mafic layers.
Analyst: E. Jarosewich, U. S. National Museum, Washington, D. C.

from areas where magmatic-type mafic layers are rare or absent. The peridotite which is associated with magmatic-type mafic layers is relatively depleted in Si, Al, Ca, Na, and S and relatively enriched in Mg and Fe. Although there are only three analyses in this diagram the general association of dunites or harzburgites with magmatic layers and the variation of olivine and orthopyroxene compositions (discussed below) suggest that the pattern is significant.

3. *Discussion of compositional variations.* The variation of magmatic mafic layer compositions could be explained by fractional crystallization: similar sympathetic variations of Ca, Al and the alkalies are found in some basic differentiated bodies such as the Prospect alkaline diabase-picrite intrusion (Wilshire, 1967). The variation of peridotite compositions, however, is not easily explained by fractional crystallization, for instead of approaching the mafic layers in composition, the peridotite which is closest to them physically is farthest from them chemically—with the important exception of Fe.

Both the variations of peridotite and magmatic-type mafic layers are compatible with an hypothesis involving partial fusion of mantle rock.

4. *Partial fusion hypothesis.* If a mass of mantle rock is displaced upwards by a convective or other force, it will follow a gradient between the adiabatic gradient and the geothermal gradient (Fig. 15a). Eventually the rising mantle rock may pierce its solidus and begin to melt. As long as all of the original solid phases are present and the pressure remains constant the composition of the melt will not change. If, however, pressure decreases during melting the composition of the melt will change. During gradual decompression at nearly constant temperature it seems probable that the melt's Mg:Fe and Ca:Na ratios will increase and the concentrations of Ti (MacGregor, 1966) and Al in the melt will decrease. These changes will be gradual, but as soon as one of the solid phases is consumed the composition of the melt will begin to change more rapidly. Diopside is probably the first phase to disappear, and when it does the melt will soon become enriched in Mg relative to Ca, Al and alkalies. If liquid and solid remain in equilibrium the change in melt composition will be continuous. If the liquid is removed, however, the next melt from the solid residue will be quite different in composition. The latter process has been called fractional fusion (Presnall, 1969).

As the peridotite mass rises, it deforms and the droplets of melt are smeared out. As deformation continues, the droplets coalesce into closely spaced, thin sheets, parallel to the flow lines of the deforming peridotite. With prolonged deformation the thin sheets coalesce, forming thicker, more widely spaced layers.

The melting peridotite becomes depleted in those elements which are concentrated in the melt, namely: Si, Al, Ca, alkalies, Mn and Fe. Why then is R131 enriched in Fe relative to the peridotites (R224, R243), which appear to

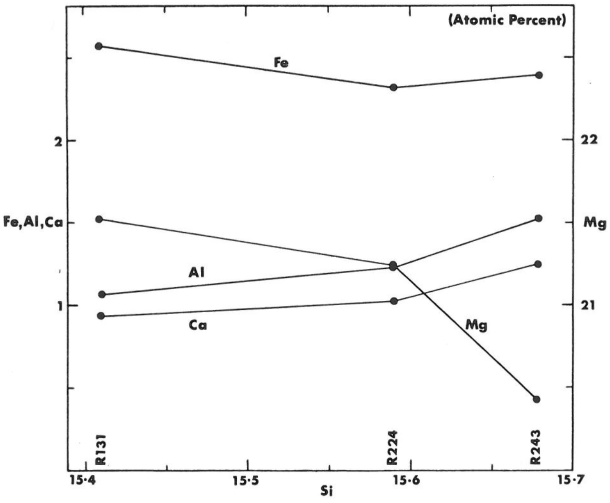

FIG. 14. Variation diagram, atomic percent Al, Ca, Fe, and Mg vs atomic percent Si, for peridotites of the Serrania de la Ronda. R131 was collected from a section of interlayered peridotite and magmatic-type mafic layers, 45 cm from the nearest mafic layer. R224 and R243 were collected from outcrops with no magmatic-type mafic layers.

have undergone little or no fusion? As the layers grow, equilibrium between the melt and the residual solid can only be approached along a decreasing number of interfaces. Along these interfaces the olivines and orthopyroxenes in the peridotite become richer in Fe as the peridotite cools. The olivines and orthopyroxenes in the more distant peridotite, however, are no longer in communication with the magma and can not become more ferruginous as the mass cools.

Returning to the compositions of magmatic-type mafic layers in the Ronda massif and applying the partial fusion interpretation to Figure 13: the compositions with the highest Fe:Mg ratios may represent the highest pressure melts. As the mass rose and the pressure decreased, the composition of the melt changed gradually, producing gentle slopes on the variation diagram. When a solid phase, probably clinopyroxene, was exhausted the composition of the melt changed rapidly and new, radically different, liquids might have appeared. This may account for the sharp breaks on the low Fe:Mg side of Figure 13 and the presence of moritic magmatic layers (Table 1, analysis h).

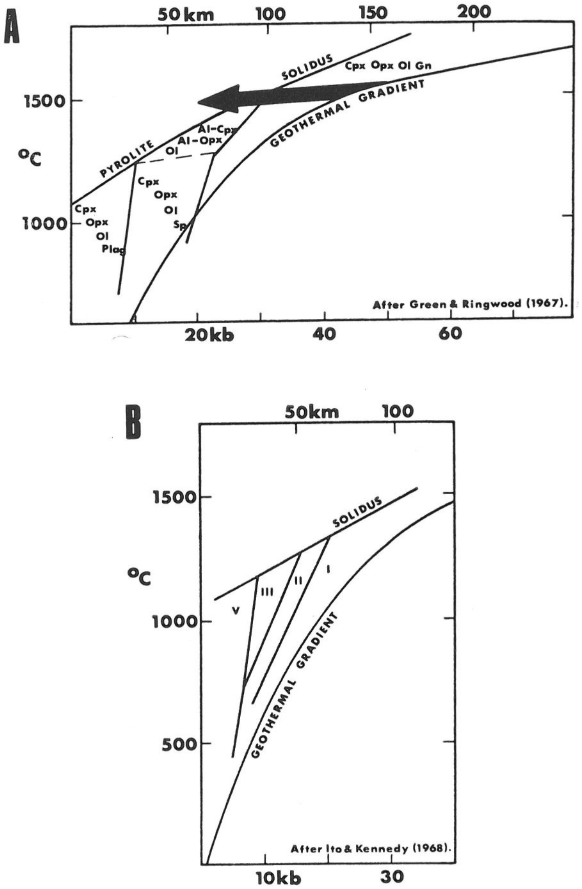

After Green & Ringwood (1967).

After Ito & Kennedy (1968).

FIG. 15. Mantle rock, rising adiabatically from some point on the geothermal gradient, would follow a *P-T* trajectory parallel to the arrow in Fig. 15A. The stability fields in 15A are for the pryolite composition (Green and Ringwood, 1967b). Eventually the rising mantle rock might pierce its solidus and begin to melt. The mineral assemblages which crystallized from such a melt would depend upon its composition and the relative rates of cooling and decompression. Approximate stability fields for the assemblages: I = gn+cpx, II = cpx+gn+plag ± opx, III = cpx+plag+opx ± sp, V = ol+cpx+plag+opx (based upon an extrapolation by Ito and Kennedy (1968) for an olivine tholeiite) are shown in Fig. 15B.

There is a rough correlation between geographic distribution, mineral assemblage, and composition of the magmatic layers: two of the three highest Fe:Mg ratios are from garnet and spinel pyroxenites. Perhaps the Ronda mass rose east end first.

Eventually the rising peridotite mass cooled and the layers of magma crystallized. The sequence of mineral assemblages observed in the Ronda massif is nicely accommodated in Figure 15b. This diagram was constructed by Ito and Kennedy (1968) for a basaltic composition, so the numbers will not apply precisely to the magmatic-type mafic layers. The relative positions of the stability fields, however, are probably correct. In the Ronda mafic layers it is difficult to determine which assemblages crystallized directly from magmas and which are retrograde from higher pressure assemblages. I suspect that there were primary garnet pyroxenites, spinel pyroxenites, and olivine gabbros, yet many of the textures described earlier and mineral compositions, presented below, indicate that a substantial amount of subsolidus recrystallization has taken place.

Mineral Compositions

1. *Olivine.* Olivine compositions from Etang de Lers, Serrania de la Ronda, Beni Bouchera, and Vourinos peridotite bodies (Fig. 16) show that olivines from peridotite near magmatic-type mafic layers tend to be richer in Fe than olivines from peridotites with no adjacent mafic layers. Olivines from magmatic-type mafic layers are considerably richer in Fe.[1]

2. *Plagioclase.* Plagioclases from magmatic layers in the Ronda massif (Fig. 17) are andesines (An_{39-40}) in assemblage II and labradorite-bytownites (An_{65-88}) in assemblages III to V. The latter are twinned (albite and ala B laws) and often zoned. In layers of assemblage IV, plagioclase growing at the expense of aluminous pyroxenes and spinel is typically zoned with Ca increasing outwards. From assemblages III to V plagioclase becomes more calcic as it increases in abundance. These observations are in accord with Green's and Ringwood's experiments (1967a) in which they found that from 10 to 18 kbar Al is increasingly soluble in clinopyroxene as (Ca, Mg)Al_2SiO_6 but not as $NaAlSi_2O_6$ until 18 to 20 kbar.

---

[1] Examination of the Vourinos massif of northern Greece by the author and Dr. Eldridge Moores revealed no magmatic-type mafic layers in the peridotite. The peridotite is overlain by mafic dikes and lavas, and if mafic magmas were produced by partial fusion of the peridotite they may have escaped to form the overlying igneous rocks rather than forming internal mafic layers. The Mg-rich olivines from the Vourinos peridotite are compatible with this interpretation.

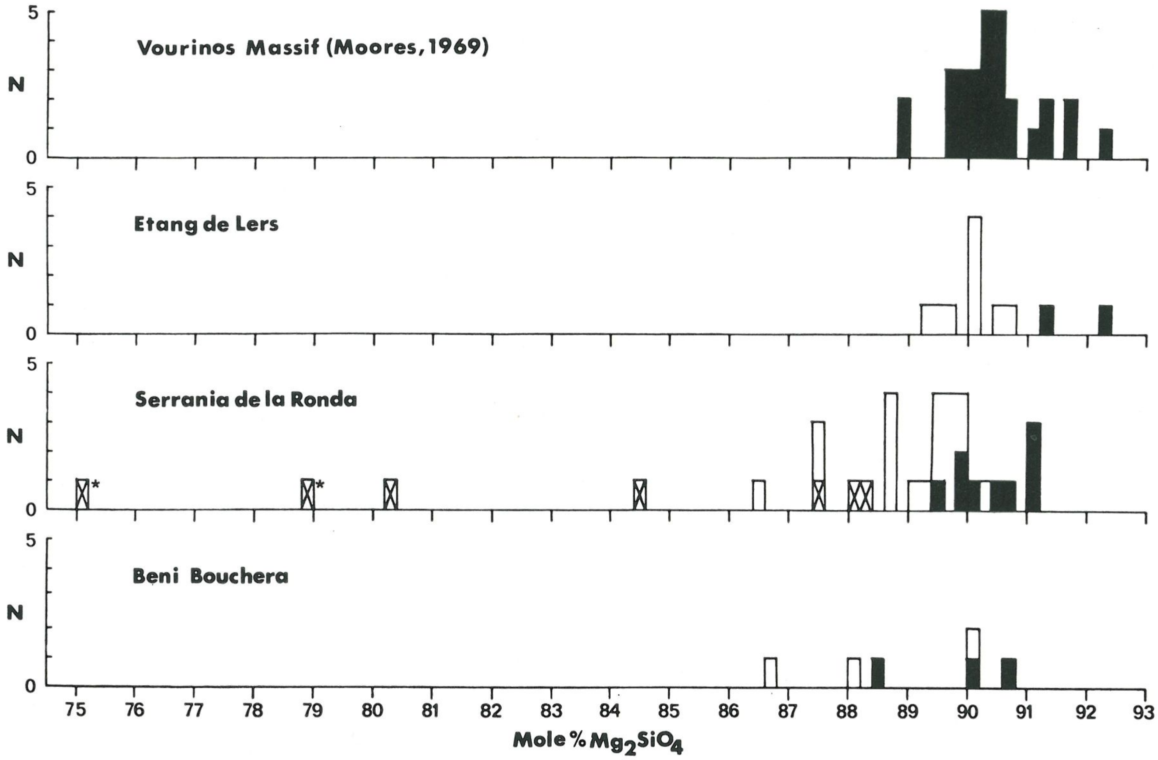

FIG. 16. Compositions of olivines from peridotite with no magmatic-type mafic layers (black), peridotite with magmatic-type mafic layers (white), and magmatic-type mafic layers (×). (*) indicates determinations by X-ray diffraction method of Yoder and Sahama (1957); all others by X-ray diffraction method of Hotz and Jackson (1962), except one chemically analyzed olivine (Fo_{92}) from Etang de Lers (Collée, 1962). Class interval = 0.2 mole %.

The sodic nature of the plagioclase coexisting with garnet in assemblage II is due in part to the readiness of garnet to include Ca but not Na. It should be noted, however, that the one analyzed rock of this assemblage (R127) contains more Na than other analyzed layers from the Ronda massif.

3. *Pyroxenes.* Like olivine, pyroxenes in magmatic-type mafic layers generally contain more Fe than those in peridotite, and pyroxenes in peridotite near magmatic-type mafic layers contain more Fe than those in peridotite which lacks magmatic layers.

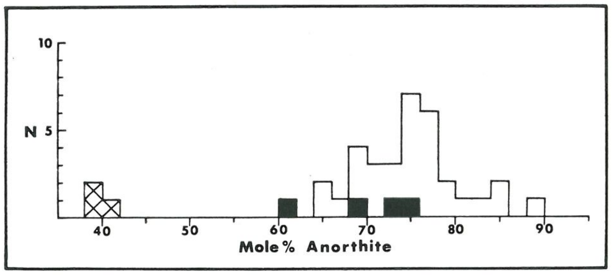

FIG. 17. Compositions of plagioclases in garnetiferous magmatic-type mafic layers (×), nongarnetiferous magmatic-type mafic layers (white), and peridotite (black). All specimens from the Serrania de la Ronda. All determinations are by refractive index. Class interval = 2 mole %.

The distribution of Ca between coexisting ortho- and clinopyroxenes in the Ronda massif (Fig. 18) suggests that they last equilibrated on the pyroxene solvus (Boyd and Schairer, 1964; Davis and Boyd, 1966) below 1000°C. This of course, corroborates the textural evidence for subsolidus recrystallization.

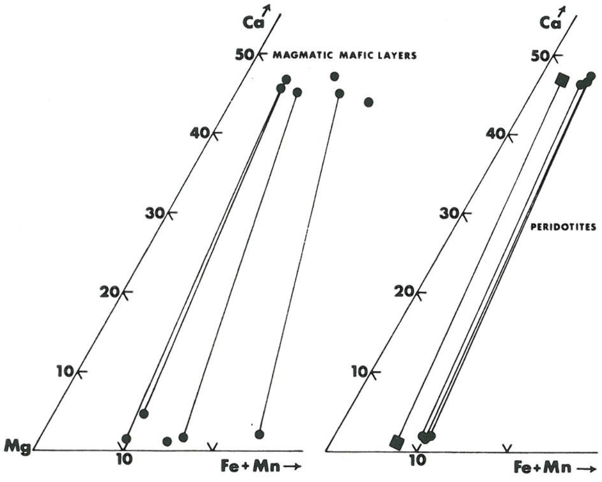

FIG. 18. CFM plot (atomic percent) for pyroxenes from magmatic-type mafic layers, peridotites, and a websterite (squares), from the Serrania de la Ronda. Analyses by electron microprobe.

Pyroxenes of the Ronda massif vary considerably in Al content (Fig. 19). In the magmatic-type mafic layers the Al content of the pyroxenes decreases markedly between assemblages III and V. The Al is present chiefly in Tschermak substitution ([Ca,Mg]Al_2SiO_6) not as jadeite. Orthopyroxene typically contains less Al than the coexisting clinopyroxene. Clinopyroxenes of assemblages II (gn+plag+cpx±sp) and III (cpx+plag+sp±opx) appear to contain excess Al. There is a Si deficiency in their analyses (Table 3, analyses b, c) which suggests solution of (Mg,Fe)Al_2O_4 in the pyroxene. Spinel exsolution is present in clinopyroxenes of assemblage III and IV, but the clinopyroxenes of assemblage II are optically homogeneous.

Pyroxenes in the analyzed websterite layer (P301) are less aluminous than analyzed pyroxenes from the peridotite (R131, R224, R243) which indicates that the websterite is not a tectonic-type mafic layer. Similar low Al pyroxenes are present in R343, a magmatic-type mafic layer of assemblage V (cpx+opx+ol+plag+chr). The pyroxenes in R343 are also present in the same proportions ($\simeq$2 cpx:1 opx) as they are in R301. The websterite may be an adcumulate rock, formed from a magmatic layer similar in composition to R343, under moderate to low pressure (<10 kbar), by precipitation of pyroxenes plus chromite and removal of the residual liquid. The bulk composition of such an adcumulate would be approximately 53 percent SiO_2, 2 percent Al_2O_3, 1 percent Cr_2O_3, 7 percent FeO, 23 percent MgO, and 15 percent CaO, which compares well with the bulk composition of R301 (Table 1, analysis i).

4. *Garnet.* Garnets in magmatic-type mafic layers (Table 4) are dominantly pyrope-almandine solutions. The pyrope content is typically higher in assemblage I than in assemblage II.

The analyzed garnets from Etang de Lers and Ronda are nearly homogeneous. Fe enrichment outwards was found in a garnet from assemblage II at Ronda, but the difference between the core and the edge of the crystal was only 1 percent FeO.

5. *Spinel.* Spinel is present in many magmatic-type mafic layers and shows distinctive changes in composition (Table 5) from assemblages I to V. The spinels in assemblages I, II, and III are green ceylonites, rich in (Mg, Fe) Al_2O_4. In assemblage IV, which is transitional between spinel pyroxenite (III) and olivine gabbro (V), the spinels change from green ceylonites to brown picotites to opaque chromite as Al, Fe^{2+}, and Mg are extracted to form plagioclase and olivine (*cf.* equation 5).

DISCUSSION

Magmatic-type mafic layers are not a common feature of alpine-type peridotite bodies. Apparently tectonic conditions often permit the liquids to escape, some to crystallize as hypabyssal intrusives, others eventually to erupt. In this way an ophiolite association of lavas and dikes overlying peridotite could be formed. By no coincidence, I think, magmatic-type mafic layers are rare in peridotites of ophiolite assemblages. Nevertheless, there are descriptions in the literature of peridotite bodies which may contain magmatic as well as tectonic-type mafic layers. Examples are the peridotites of Cabo Ortegal, Totalp, and Sondmör:

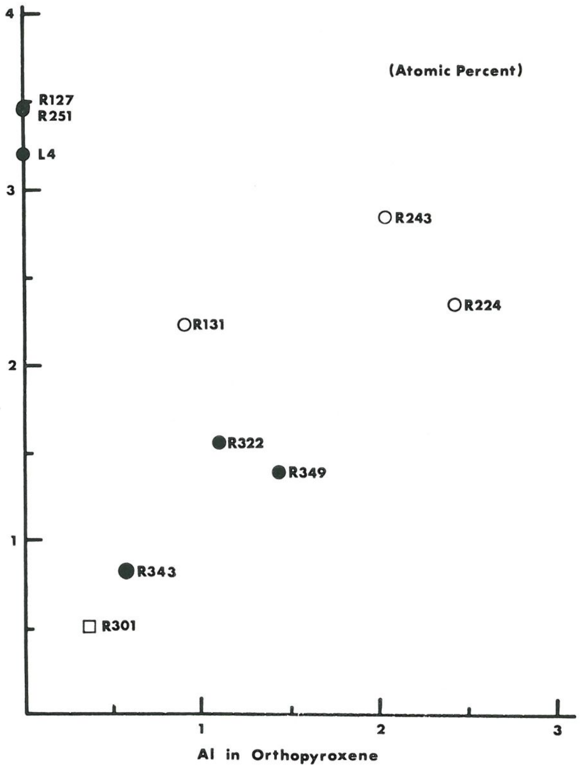

FIG. 19. Al in coexisting ortho- and clinopyroxenes from magmatic-type mafic layers (solid circles), peridotites (open circles), and a websterite (square) of the Serrania de la Ronda. Also shown are clinopyroxenes from a garnet plagioclase pyroxenite (R127) and a spinel pyroxenite (R251) from Ronda and a garnet pyroxenite (L4) from Etang de Lers. Magmatic-type mineral assemblages are: (I) L4, (II) R127, (III) R251, (IV) R322 & R349, (V) R343. L4 analyzed by E. Jarosewich; others by electron microprobe.

Cabo Ortegal (*N. W. Spain*)

Serpentinized peridotite bodies in a high-grade metamorphic terrane at Cabo Ortegal, N. W. Spain (Vogel. 1967) contain deformed veins (up to 5 cm wide) of spinel +garnet pyroxenite. Despite the intense metamorphism these pyroxenites are mineralogically and chemically similar to magmatic-type mafic layers.

Totalp (*Switzerland*). The Totalp serpentinite body, near Davos, Switzerland (Peters 1963, 1968) is a serpentinized lherzolite containing layers (2 to 40/cm thick) of picotite pyroxenite, ceylonite and ceylonite+pyrope pyroxenite, and spinel-free pyroxenite. The ceylonite pyroxenites and ceylonite+pyrope pyroxenites resemble magmatic-type mafic layers of assemblages I and III. The picotite pyroxenites and spinel-free pyroxenites may also be magmatic-type mafic layers, or they may be tectonic layers. The

Table 3. Compositions of Pyroxenes in Mafic Layers and Associated Peridotites

	a	b	c	d	e	f	g	h	i	j	k	l	m	n	o	p	q	r	s	t
Type	*M*(I)	*M*(II)	*M*(III)	*M*(IV)	*M*(IV)	*M*(IV)	*M*(IV)	*M*(IV)	*M*(IV)	*M*(IV)	*M*(V)	*M*(V)	*T*	*T*	*P*	*P*	*P*	*P*	*P*	*P*
SiO_2	51.87	47.9(6)	47.4(3)	50.3(4)	53.7(4)	53.8(8)	53.8(0)	54.5(2)	51.4(8)	55.4(5)	53.1(2)	55.4(8)	55.7(0)	57.6(3)	50.0(5)	55.5(7)	53.6(2)	54.4(8)	51.2(4)	53.7(0)
TiO_2	0.13	1.3(2)	1.5(2)	0.4(7)	0.1(3)	0.3(9)	0.8(5)	0.3(6)	0.1(9)	0.05	0.1(3)	0.05	0.06	0.02	1.5(2)	0.4(2)	0.4(3)	0.08	0.5(7)	0.1(7)
Al_2O_3	7.52	7.9(1)	7.8(8)	6.4(7)	2.8(3)	2.2(4)	3.6(5)	2.6(9)	3.2(4)	3.6(1)	1.9(1)	1.3(8)	1.2(1)	0.9(3)	5.2(6)	2.3(0)	5.5(5)	6.0(3)	6.6(7)	5.0(6)
Cr_2O_3	0.20	0.1(0)	0.04	0.2(0)	0.1(3)	0.1(9)	0.5(9)	0.3(6)	1.5(4)	0.9(9)	0.6(6)	0.3(9)	1.6(6)	0.5(6)	1.2(7)	0.5(1)	1.0(9)	0.7(0)	0.9(0)	0.5(7)
Fe_2O_3	0.94	—	—	—	—	—	—	—	—	—	—	—	—	—	—	—	—	—	—	—
FeO	2.08	8.4(7)	5.5(3)	6.5(2)	16.4(3)	9.5(4)	2.6(0)	6.5(7)	2.7(7)	6.4(0)	4.2(2)	10.3(8)	1.5(3)	4.9(5)	3.1(6)	6.7(4)	2.6(1)	6.0(8)	2.7(8)	6.9(7)
MnO	0.04	0.1(5)	0.1(9)	0.2(3)	0.4(0)	0.3(8)	0.1(7)	0.2(9)	0.1(0)	0.1(9)	0.1(8)	0.3(4)	0.1(2)	0.1(5)	0.1(0)	0.1(9)	0.09	0.2(0)	0.1(1)	0.2(0)
MgO	14.32	13.0(0)	13.8(7)	14.5(8)	29.0(1)	33.2(8)	16.1(1)	33.0(0)	17.5(0)	31.8(8)	17.2(1)	30.6(8)	17.7(0)	34.9(1)	16.5(4)	33.2(5)	15.6(6)	32.6(4)	14.6(3)	33.5(4)
CaO	21.25	19.3(9)	21.0(9)	20.9(0)	1.1(0)	0.6(4)	21.7(3)	2.5(7)	22.5(0)	0.7(1)	22.3(8)	1.0(2)	23.0(2)	0.4(5)	22.4(1)	0.8(3)	20.7(3)	1.0(0)	20.5(2)	1.1(0)
Na_2O	1.42	1.3(4)	0.9(5)	9.7(3)	0.00	0.03	0.5(2)	0.01	0.5(6)	0.00	0.3(7)	0.00	0.7(6)	0.03	0.8(6)	0.01	0.7(7)	0.03	2.2(6)	0.2(0)
K_2O	0.01	0.00	0.00	0.00	0.00	0.01	0.01	0.00	0.00	0.00	0.00	0.00	0.02	0.00	0.01	0.00	0.00	0.01	0.01	0.01
Total	99.87*	99.65**	98.50	100.45	103.77	100.59	100.03	100.39	99.90	99.28	100.18	99.72	101.81	99.63	101.19	99.82	100.55	101.28	99.71	101.51
Analyses in terms of 6 Oxygens																				
Si	1.874	1.791	1.778	1.847	1.882	1.889	1.943	1.897	1.884	1.931	1.940	1.961	1.980	1.983	1.815	1.931	1.920	1.861	1.868	1.845
Al (IV)	0.126	0.209	0.222	0.153	0.117	0.093	0.057	0.103	0.116	0.069	0.060	0.039	0.020	0.017	0.185	0.069	0.080	0.139	0.132	0.155
Al (VI)	0.194	0.139	0.125	0.126	0.000	0.000	0.098	0.007	0.024	0.079	0.023	0.019	0.031	0.020	0.040	0.025	0.155	0.104	0.154	0.050
Ti	0.004	0.037	0.043	0.013	0.003	0.010	0.023	0.009	0.005	0.001	0.003	0.001	0.002	0.001	0.041	0.011	0.012	0.002	0.016	0.004
Cr	0.004	0.003	0.001	0.006	0.004	0.005	0.017	0.010	0.045	0.027	0.019	0.011	0.047	0.015	0.037	0.014	0.031	0.019	0.026	0.015
Fe^3	0.025	—	—	—	—	—	—	—	—	—	—	—	—	—	—	—	—	—	—	—
Fe^2	0.062	0.265	0.173	0.200	0.481	0.280	0.079	0.191	0.085	0.186	0.129	0.307	0.046	0.142	0.096	0.196	0.078	0.174	0.085	0.200
Mn	0.012	0.005	0.006	0.007	0.012	0.011	0.005	0.008	0.003	0.006	0.005	0.010	0.004	0.004	0.003	0.006	0.003	0.006	0.003	0.006
Mg	0.771	0.724	0.775	0.797	1.514	1.739	0.867	1.711	0.954	1.655	0.937	1.617	0.938	1.790	0.894	1.722	0.836	1.662	0.795	1.717
Ca	0.822	0.776	0.847	0.821	0.041	0.024	0.841	0.096	0.882	0.027	0.876	0.039	0.877	0.017	0.871	0.031	0.795	0.037	0.801	0.041
Na	0.099	0.097	0.069	0.052	0.000	0.002	0.036	0.001	0.040	0.000	0.026	0.000	0.052	0.002	0.060	0.001	0.053	0.002	0.160	0.013
Total	3.994	4.046	4.039	4.022	4.054	4.053	3.966	4.033	4.038	3.981	4.018	4.004	3.997	3.991	4.042	4.006	3.963	4.006	4.040	4.046

Key to Table 3

Type: *M* =magmatic, *T* =tectonic, *P* =peridotite, Roman numerals stand for mineral assemblages.

*Analysis includes 0.10% H_2O^+, 0.06% H_2O^-, 0.04% NiO, less than 0.01% P_2O_5.

**Analyses b through t by electron microprobe. Oxygen determined by stoichiometry, assuming all Fe as FeO. All specimens from Serrania de la Ronda, Spain.

a. Clinopyroxene in garnet-spinel pyroxenite, L4, Etang de Lers, France. Analyst: E. Jarosewich.
b. Clinopyroxene in garnet-plagioclase pyroxenite, R127.
c. Clinopyroxene in spinel-plagioclase pyroxenite, R251.
d. Clinopyroxene in gabbro, R183.
e. Orthopyroxene in gabbro, R183.
f. Clinopyroxene in olivine gabbro, R120.
g. Clinopyroxene in olivine gabbro, R322.
h. Orthopyroxene in olivine gabbro, R322.
i. Clinopyroxene in olivine gabbro, R349.
j. Orthopyroxene in olivine gabbro, R349.
k. Clinopyroxene in olivine gabbro, R343.
l. Orthopyroxene in olivine gabbro, R343.
m. Clinopyroxene in websterite, R301.
n. Orthopyroxene in websterite, R301.
o. Clinopyroxene in harzburgite, R131.
p. Orthopyroxene in harzburgite, R131.
q. Clinopyroxene in harzburgite, R224.
r. Orthopyroxene in harzburgite, R224.
s. Clinopyroxene in lherzolite, R243.
t. Orthopyroxene in lherzolite, R243.

picotite pyroxenites have lower Al content and Fe:Mg ratios than most magmatic-type layers.

Sondmör District (*Norway*). Peridotite bodies in Caledonian gneisses near Tafjord and Almklovdalen, Norway (Eskola, 1921; Carswell, 1968), contain lenses of garnet pyroxenite which appear to be magmatic-type mafic layers. In these rocks there is no clean division between garnet pyroxenites and peridotites. Bulk compositions vary continuously from pyroxenite to peridotite, and Carswell (1968) has determined that the variation can be expressed in terms of two compositions which are approximated by serpentinized dunite and garnet pyroxenite. He concludes that the garnet pyroxenites probably formed by partial fusion, leaving dunite as the unmelted residue.

The origin of these mafic layers which I have referred to as the magmatic-type has been explained in various ways: Thayer (1963) has interpreted similar features as magmatic flow layering, formed during movement of a magmatically differentiated, crystal mush. O'Hara and Mercy (O'Hara, 1967) have suggested that the Etang de Lers and other Pyrenean lherzolites are metamorphosed accumulates. Peters (1963) has suggested that the mafic layers in the Totalp serpentinite represent the last liquids to crystallize from a peridotite magma. These interpretations are all based upon the process of fractional crystallization.

Table 4. Garnets from Magmatic-Type Mafic Layers in the Etang de Lers and Serrania de la Ronda Peridotites

			Cations per 12 Oxygens		
	a	b		a	b
Type	I	II			
SiO_2	41.70	41.4(6)	Si	2.987	3.051
TiO_2	0.06	0.2(2)	Al^{IV}	0.013	—
Al_2O_3	23.33	21.9(2)	Al^{VI}	1.957	1.901
Cr_2O_3	0.18	0.1(0)	Ti	0.003	0.012
Fe_2O_3	1.31	—	Fe^3	0.071	—
FeO	9.98	15.4(7)[a]	Cr	0.010	0.006
MnO	0.32	0.4(9)	Mg	1.879	1.471
MgO	17.59	13.4(1)	Ni	—	—
CaO	5.78	7.0(6)	Fe^2	0.598	0.952
Na_2O	0.03	0.03	Mn	0.019	0.031
K_2O	0.01	0.00	Ca	0.444	0.557
H_2O^+	0.10	—	Na	0.004	0.004
H_2O^-	0.03	—	K	—	0.000
P_2O_5	0.01	—	P	—	—
NiO	0.01	—			
Total	100.31	100.18	Total	7.985	7.985

[a] Total Fe as FeO.

Key to Table 4

Roman numerals refer to mineral assemblages.

a. Garnet in garnet pyroxenite, L4, Etang de Lers, France. Analyst: E. Jarosewich.

b. Garnet in garnet-plagioclase pyroxenite, R127, Serrania de la Ronda, Spain. Analysis by electron microprobe. Oxygen calculated stoichiometrically, assuming all Fe as FeO.

Table 5. Spinels from Magmatic-Type Mafic Layers in the Serrania de la Ronda Peridotite

	a	b	c	d
Assemblage	III	IV	IV	V
Ti	0.09	—	0.1(0)	0.1(0)
Al	31.6(8)	31.1(3)	30.7(1)	15.1(4)
Cr	0.2(2)	2.7(6)	4.7(0)	19.8(1)
Fe	17.4(3)	12.4(4)	9.9(6)	23.4(2)
Mn	0.1(8)	0.1(6)	0.1(2)	0.4(2)
Mg	10.7(4)	12.7(8)	13.1(3)	5.7(8)
O[a]	40.8(5)	41.4(5)	41.4(8)	35.5(4)
Total	101.19	100.72	100.20	100.22
Compositions in terms of Spinel-Type Molecules				
$MgAl_2O_4$	68.5	80.5	83.1	44.4
$MnAl_2O_4$	0.5	0.5	0.3	1.4
$FeAl_2O_4$	22.0	7.4	4.1	6.6
$FeCr_2O_4$	0.3	4.1	7.0	35.6
$FeFe_2O_4$	8.7	7.5	5.5	12.0

[a] Oxygen determined by stoichiometry, assuming Fe combined as FeO for analyses a,b,c and as Fe_3O_4 for analysis d.

Key to Table 5

Roman numerals stand for mineral assemblages.

a. Spinel in spinel pyroxenite, R251.

b. Spinel in olivine gabbro, R120.

c. Spinel in olivine gabbro, R322.

d. Spinel in olivine gabbro, R343.

Analyses by electron microprobe.

In terms of chemistry and mineralogy the Ronda massif, which is large, well-exposed, and relatively fresh, bears little resemblance to a product of fractional crystallization. Peridotite composition does vary with the abundance of magmatic-type mafic layers, but rather than being enriched in Si, Al, Ca, and alkalies, the peridotite near the magmatic-type mafic layers is depleted in those elements. The magmatic-type mafic layers also vary in bulk composition, but those which are richest in Al, Ca, Fe, alkalies and Ti are of the higher pressure assemblages, spinel and garnet pyroxenites, which apparently crystallized deeper than the gabbroic layers.

The relationships in the Ronda massif can be explained in terms of partial fusion of a rising mass of peridotite with subsequent crystallization and recrystallization along a decreasing $P-T$ gradient. The bulk compositions of the magmatic-type mafic layers are, in fact, quite similar to the picritic compositions which several experimentalists (*eg.* Davis and Schairer, 1965, O'Hara and Yoder, 1967; Ito and Kennedy, 1967) suggest for the early melting fraction of peridotite at high pressure.

If the partial fusion hypothesis is correct, then the magmatic-type mafic layers are of considerable importance in clarifying the origin and evolution of basalts. Within the

TABLE 6

	a	b	c	d	e
SiO_2	44.28	44.62	44.77	44.93	45.16
TiO_2	0.18	0.14	0.19	0.08	0.71
Al_2O_3	4.90	3.66	4.16	3.21	3.54
Cr_2O_3	0.33	0.33	0.40	0.45	0.43
Fe_2O_3	1.65	0.59			0.46
FeO	7.01	7.58	8.21[a]	7.58[a]	8.04
MnO	0.13	0.13	0.11	0.14	0.14
MgO	36.65	38.98	39.22	40.03	37.47
CaO	4.29	3.31	2.42	2.99	3.08
Na_2O	0.35	0.26	0.22	0.18	0.57
K_2O	0.01	0.00	0.05	0.02	0.13
P_2O_5	0.00	0.00	0.01	—	0.06
NiO	0.23	0.27	0.24	0.26	0.20
CoO	—	—	—	—	0.01
	100.00	99.99	100.00	99.87	100.00

[a] Total Fe as FeO.

Key to Table 6

a. Ronda average (85% R131+15% R183).
b. Lherzolite, R243, calculated H_2O-free.
c. Lizard average (Green, 1964).
d. Tinaquillo peridotite (MacKenzie, 1960).
e. Pyrolite (Ringwood, 1966).

Ronda massif, which is 38 km long, there are both hypersthene normative and nepheline normative magmatic layers. If these magmatic layers represent protobasaltic magmas, from which basalts are descended, perhaps the depths of origin of the alkali olivine basalts and the tholeiites are not very different. Perhaps the depth at which magmas are released from the melting peridotite, (Green's and Ringwood's (1967a) depth of magma segregation), is in fact decisive in determining the kind of basalt which may erupt.

The clarity of field relationships at Ronda provides an opportunity to estimate the composition of the parental peridotite. This estimate is made by combining the peridotite (R131) which occurs with magmatic-type mafic layers with an appropriate magmatic layer (R183) in the proportions (85:15) in which peridotite and magmatic layers occur in the area from which both specimens were collected. The estimated original composition (Table 6, analysis a) approaches the composition of R243 (analysis b) which appears to be the least depleted of the analyzed Ronda peridotites. Also similar are the compositions of two other high-temperature peridotites, the Lizard and Tinaquillo (analyses c, d). Not surprisingly, the pyrolite composition (Ringwood, 1966) (analysis e) is also similar.

CONCLUSION

Magmatic-type mafic layers are distinctive constituents of some alpine-type peridotite bodies. Field relations show that they are indigenous to the peridotite bodies and suggest that they grow by a form of flow differentiation in largely (70 to 90%) crystalline bodies. The structural simplicity displayed by magmatic layers in many bodies, particularly the Ronda massif, suggests that when the layers were formed the peridotite was deforming uniformly on a fairly large scale (of the order of kilometers).

The variation of peridotite compositions in the Ronda massif is, in view of the field relationships of the samples, difficult to explain by fractional crystallization. A partial fusion process, on the other hand, explains both the observed variations of the peridotite and the magmatic mafic layer compositions.

If the partial fusion hypothesis is correct, magmatic-type mafic layers may be reliable representatives of protobasaltic magmas and, as such, will be of considerable interest to students of basalt genesis.

ACKNOWLEDGEMENTS

The late Professor Harry H. Hess was my principal advisor during this research. I am grateful for his generous support, wise counsel, and friendship.

The following friends and colleagues were particularly helpful: Dr. H. G. Avé Lallemant, Professor J. M. Fontboté, Professor R. B. Hargraves, Dr. J. Kornprobst, Mr. R. J. G. Lewis, Professor J. B. Lyons, Professor J. C. Maxwell, Professor E. Moores, Dr. J. A. Wood, and Dr. H. S. Yoder, Jr.

Chemical analyses were performed at the U. S. National Museum by Mr. E. Jarosewich.

Research facilities were provided by the Department of Geological and Geophysical Sciences of Princeton University and the Smithsonian Astrophysical Observatory.

This research was supported by an N.A.S.A. Trainee Fellowship, a Kennecott Corporation Fellowship, N.S.F. Grant GA-408 (H. H. Hess and J. C. Maxwell, Principal Investigators), and my parents.

Joan E. Dickey was my field and laboratory assistant.

REFERENCES

AVÉ LALLEMANT, H. G. (1967) Structural and petrofabric analysis of an "alpine-type" peridotite: the lherzolite of the French Pyrenees. *Leidse Geol. Med.* **42,** 1–57.

BENSON, W. N. (1926) The tectonic conditions accompanying the intrusion of basic and ultrabasic igneous rocks. *U. S. Acad. Sci. Mem.* **1,** 1–90.

BOWEN, N. L. (1928) *The Evolution of the Igneous Rocks.* Princeton University Press, Princeton, New Jersey.

BOYD, F. R., JR., AND J. F. SCHAIRER (1964) The system $MgSiO_3$-$CaMgSi_2O_6$. *J. Petrology* **5,** 275–309.

CARSWELL, D. A. (1968) Picritic magma-residual dunite relationships in garnet peridotite at Kalskaret near Tafjord, South Norway. *Contrib. Mineral. Petrology* **19,** 97–124.

COLLÉE, A. L. G. (1962) A fabric study of lherzolites, with special reference to ultrabasic nodular inclusions in the lavas of Auvergne (France). *Leidse Geol. Med.* **28,** 3–102.

DAVIS, B. T. C., AND F. R. BOYD, JR. (1966) The join $Mg_2Si_2O_6$-$CaMgSi_2O_6$ at 30 kilobars pressure and its application to pyroxenes from kimberlites. *J. Geophys. Res.* **71,** 3567–3576.

———, AND J. F. SCHAIRER (1965) Melting relations in the join diopside-forsterite-pyrope at 40 kilobars and at one atmosphere. *Carnegie Inst. Wash. Year Book* **64,** 123–134.

DE LÁMTHERIE, J. C. (1795) *Théorie de la Terre. Tome 1.* Paris, 464.

DE SITTER, L. U. (1956) *Structural Geology.* McGraw-Hill Book Co. Inc., New York, 552.

ESKOLA, P. (1921) On the eclogites of Norway: *Vidensk.-selsk.*

Skr., Kristiana, I. Mat.-Naturvid. Kl., **8**, 1–118.

Fallot, P. (1948) Les cordillères bétique. *Cons. Sup. Invest. Cient., Inst. Lucas Mallada* **8**, 83–172.

Fontboté, J. M. (1966) Esquema estructural de las cordilleras beticas. *Inst. Geol. Mineral España, Libreria Parainfo.*

Gibb, F. G. F. (1968) Flow differentiation in the xenolithic ultrabasic dykes of the Cuillins and the Strathaird Penninsula, Isle of Skye, Scotland. *J. Petrology* **9**, 411–443.

Green, D. H. (1964) The petrogenesis of the high-temperature peridotite intrusion in the Lizard area, Cornwall. *J. Petrology* **5**, 134–188.

———, and A. E. Ringwood (1967a) The genesis of basaltic magmas. *Contrib. Mineral. Petrology* **15**, 103–190.

———, and ——— (1967b) The stability fields of aluminous pyroxene peridotite and garnet peridotite and their relevance in upper mantle structure. *Earth Planet. Sci. Lett.* **3**, 151–160.

Hess, H. H. (1955) Serpentines, orogeny, and epeirogeny. *Geol. Soc. Amer. Spec. Pap.* **62**, 391–408

——— (1960) Stillwater igneous complex, Montana. *Geol. Soc. Amer. Mem.* **80**.

Hotz, P. E., and E. D. Jackson (1962) X-ray determinative curve for olivines of composition Fo_{80-95} from stratiform and alpine-type peridotites. *U. S. Geol. Surv. Prof. Pap.*, **450E**, E101–E102.

Ito, K and G. C. Kennedy, (1967) Melting and phase relations in a natural peridotite to 40 kilobars. *Amer. J. Sci.* **265**, 211–217.

———, and ——— (1968) Melting and phase relations in the plane tholeiite-lherzolite-nepheline basanite to 40 kilobars with geological implications. *Contrib. Mineral. Petrology* **19**, 177–211.

Kornprobst, J. (1966) A propos des peridotites du massif des Beni-Bouchera (Rif septentrional, Maroc). *Bull. Soc. Franc. Mineral. Cristallogr.* **89**, 399–404.

Lacroix, A. (1894) Etude mineralogique de la lherzolite des Pyrenées et ses phenomenes de contact. *Nouv. Arch. Mus. Hist. Nat. Paris* **6**, 209–308.

——— (1900) Les roches basiques accompagnant les lherzolites et les ophites des Pyrenées. *8th Int. Geol. Congr. Rept.*, 806–838.

Lovering, J. F., and A. J. R. White (1968) Granulitic and eclogitic inclusions from basic pipes at Delegate, Australia. *Contributions to the Geochemistry and Petrology of the Crust and Upper Mantle, No. 1*, Australian National Univ., Canberra, A. C. T.

MacGregor, I. D. (1966) The effect of pressure on the minimum melting composition in the system MgO-SiO_2-TiO_2 (abstr.). *Trans. Amer. Geophys. Union* **47**, 207–208.

MacKenzie, D. B. (1960) High-temperature alpine-type peridotite from Venezuela. *Geol. Soc. Amer. Bull.* **71**, 303–318.

Manson, V. (1967) Geochemistry of basaltic rocks: major elements. *In* H. H. Hess and A. Poldervaart (eds.) *The Poldervaart Treatise on Rocks of Basaltic Composition, Vol. 1.* Interscience, New York, 495.

Milliard, Y. (1959) Les massifs metamorphiques et ultrabasiques de la zone paleozoic intern du Rif. *Notes Serv. Geol. Maroc* **147**, 125–160.

Moores, E. M. (1969) Petrology and Structuie of the Vourinos Ophiolitic Complex of Northern Greece. *Geol. Soc. Amer. Spec. Pap.* **118**.

O'Hara, M. J. (1967) Garnetiferous ultrabasic rocks of orogenic regions. *In* P. J. Wyllie (ed.) *Ultramafic and Related Rocks.* John Wiley & Sons, Inc., New York, 167–172.

———, and H. S. Yoder, Jr. (1967) Formation and fractionation of basic magmas at high pressure. *Scott. J. Geol.* **3**, 67–117.

Orueta, D. (1917) Estudio geologico y petrografico de la Serrania de Ronda. *Mem. Inst. Geol. España*, 567.

Peters, Tj. (1963) Mineralogie und petrographie des Totalpserpentins bei Davos. *Schweiz. Mineral. Petrogr. Mitt.* **43**, 529–685.

——— (1968) Distribution of Mg, Fe, Al, Ca and Na in coexisting olivine, orthopyroxene and clinopyroxene in the Totalp serpentinite (Davos, Switzerland) and in the alpine metamorphosed Malenco serpentinite (N. Italy). *Contrib. Mineral. Petrology* **18**, 65–75.

Presnall, D. C. (1969) The geometrical analysis of partial fusion. *Amer. J. Sci.* **267**, 1178–1194.

Ravier, J. (1959) Le metamorphisme de terrains secondaires des Pyrenées. *Mem. Soc. Geol. France* (N.S.) **38/86**, 250.

Ringwood, A. E. (1966) The chemical composition and origin of the earth. *In* P. M. Hurley (ed.) *Advances in Earth Science.* M. I. T., Cambridge, 287–356.

Thayer, T. P. (1960) Some critical differences between alpine-type and stratiform peridotite-gabbro complexes. *Int. Geol. Congr., 21st Rept.* **13**, 247–259.

——— (1963) Flow layering in alpine peridotite-gabbro complexes. *Mineral. Soc. Amer. Spec. Pap.* **1**, 55–61.

——— (1967) Chemical and structural relations of ultramafic and feldspathic rocks in alpine intrusive complexes. *In* P. J. Wyllie (ed.) *Ultramafic and Related Rocks.* John Wiley & Sons, Inc., New York, 222–239.

Vogel, D. E. (1967) Petrology of an eclogite- and pyrigarnite-bear ing polymetamorphic rock complex at Cabo Ortegal, N. W. Spain. *Leidse Geol. Med.* **40**, 121–213.

Wager, L. R., and G. M. Brown (1967) *Layered Igenous Rocks.* W. H. Freeman & Co., San Francisco, 588.

———, and W. J. Wadsworth (1960) Types of igneous cumulates. *J. Petrology* **1**, 73–85.

Wilshire, H. G. (1967) The Prospect alkaline diabase-picrite intrusion, New South Wales, Australia. *J. Petrology* **8**, 97–163.

Yoder, H. S., Jr., and T. G. Sahama (1957) Olivine x-ray determinative curve. *Amer. Mineral.* **42**, 475-491.

———, and C. E. Tilley (1962) Origin of basalt magmas: an experimental study of natural and synthetic rock systems. *J. Petrology* **3**, 342–532.

Zwart, H. J. (1953) Sur les lherzolites et ophites des Pyrenées. *Leidse Geol. Med.* **18**, 281–286.